

The provenance of Cretaceous to Quaternary sediments in the Tarfaya basin, SW Morocco: Evidence from trace element geochemistry and radiogenic Nd–Sr isotopes



Sajid Ali^{a,*}, Karl Stattegger^a, Dieter Garbe-Schönberg^a, Martin Frank^b, Steffanie Kraft^b, Wolfgang Kuhnt^a

^a Institute of Geosciences, Christian-Albrechts-Universität, D-24118 Kiel, Germany

^b GEOMAR Helmholtz-Zentrum für Ozeanforschung Kiel, Wischhofstrasse 1-3, Kiel, Germany

ARTICLE INFO

Article history:

Received 4 July 2013

Received in revised form 22 October 2013

Accepted 14 November 2013

Available online 26 November 2013

Keywords:

Trace elements

Nd–Sr isotopes

Provenance

Tarfaya basin

ABSTRACT

We present trace element compositions, rare earth elements (REEs) and radiogenic Nd–Sr isotope analyses of Cretaceous to recent sediments of the Tarfaya basin, SW Morocco, in order to identify tectonic setting, source rocks composition and sediments provenance. The results suggest that the sediments originate from heterogeneous source areas of the Reguibat Shield and the Mauritanides (West African Craton), as well as the western Anti-Atlas, which probably form the basement in this area. For interpreting the analyzed trace element results, we assume that elemental ratios such as La/Sc, Th/Sc, Cr/Th, Th/Co, La/Co and Eu/Eu* in the detrital silicate fraction of the sedimentary rocks behaved as a closed system during transport and cementation, which is justified by the consistency of all obtained results. The La/Y–Sc/Cr binary and La–Th–Sc ternary relationships suggest that the Tarfaya basin sediments were deposited in a passive margin setting. The trace element ratios of La/Sc, Th/Sc, Cr/Th and Th/Co indicate a felsic source. Moreover, chondrite-normalized REE patterns with light rare earth elements (LREE) enrichment, a flat heavy rare earth elements (HREE) and negative Eu anomalies can also be attributed to a felsic source for the Tarfaya basin sediments. The Nd isotope model ages ($T_{DM} = 2.0\text{--}2.2$ Ga) of the Early Cretaceous sediments suggest that sediments were derived from the Eburnean terrain (Reguibat Shield). On the other hand, Late Cretaceous to Miocene–Pliocene sediments show younger model ages ($T_{DM} = 1.8$ Ga, on average) indicating an origin from both the Reguibat Shield and the western Anti-Atlas. In contrast, the southernmost studied Sebkhia Aridal section (Oligocene to Miocene–Pliocene) yields older provenance ages ($T_{DM} = 2.5\text{--}2.6$ Ga) indicating that these sediments were dominantly derived from the Archean terrain of the Reguibat Shield.

© 2013 Elsevier Ltd. All rights reserved.

1. Introduction

Siliciclastic sedimentary rocks contain important information about changes in the supply of material from different sources over time, and the geochemical compositions of such sediments have proven to be a powerful tool for reconstructing the signature of tectonic settings, the composition of the source areas and the provenance of the sediments (Wronkiewicz and Condie, 1987; McLennan, 1989; Taylor and McLennan, 1985; McLennan and Taylor, 1991; McLennan et al., 1993; Roddaz et al., 2011). The primary chemical composition of sedimentary rocks has potentially been modified by chemical weathering and sorting processes during transport, sedimentation and post-depositional diagenesis (Nesbitt et al., 1980; DePaolo, 1980, 1981; Nesbitt and Young,

1982; Middelburg et al., 1988; Nesbitt et al., 1996). We assume in this study that the ratios of trace elements such as Zr, Hf, Sc, Y, Cr, Th and Co and the rare earth elements (REEs) in the detrital silicate fraction of our sedimentary rocks have behaved as a closed system and that they were not significantly affected or modified by such processes and can thus be used to distinguish the tectonic setting and provenance of clastic sediments similar to numerous previous studies (e.g., Taylor and McLennan, 1985; Bhatia and Crook, 1986; McLennan, 1989; Zimmermann and Bahlburg, 2003; Armstrong-Altrin et al., 2004). Furthermore, Sm–Nd isotope model ages of the sedimentary rocks can be applied for distinguishing between different sources and their average crustal residence ages (e.g., McCulloch and Wasserburg, 1978; O’Nions et al., 1983; McLennan et al., 1990; McDaniel et al., 1994; Zimmermann and Bahlburg, 2003; Wade et al., 2005; Xie et al., 2012). Hence, the combination of inorganic geochemical compositions and Sm–Nd isotope model ages of such rocks, as well as their radiogenic isotope compositions provide important constraints on the tectonic settings and the

* Corresponding author. Tel.: +49 4318801177.

E-mail addresses: sa@gpi.uni-kiel.de (S. Ali), kst@gpi.uni-kiel.de (K. Stattegger), dgs@gpi.uni-kiel.de (D. Garbe-Schönberg), mfrank@geomar.de (M. Frank), skraft@geomar.de (S. Kraft), wk@gpi.uni-kiel.de (W. Kuhnt).

characteristics of the source areas at the time of their deposition. Supporting evidence can be derived from other radiogenic isotope systems such as that of Sr, which is also a sensitive indicator for the age and type of source rocks of siliciclastic sediments but is subject to variable degrees of isotopic fractionation during weathering and transport of the particles due to large variations in Sr isotope compositions of different mineral phases and thus also of different grain sizes (e.g., Tütken et al., 2002), which has to be taken into account for the interpretations.

Earlier studies in the Tarfaya basin were based on carbonate rocks from the Late Cretaceous and focused on the understanding of the intensity of anoxia, the magnitude and nature of $\delta^{13}\text{C}$ excursions, the biotic effects on benthonic and planktonic foraminifera, biostratigraphy records and the paleo-environmental evolution of the basin (e.g. El Albani et al., 1999; Kuhnt et al., 1997, 2005, 2009; Kolonic et al., 2005; Mort et al., 2007, 2008; Keller et al., 2008; Gertsch et al., 2010). Here we present results obtained from Cretaceous to recent sediments of key sections of the coastal cliffs and Sebkhas in the Tarfaya basin between Boujdour and Oued Chebeika, as well as from the upper sections of four newly drilled sediment cores. We use trace element geochemistry including rare earth elements (REEs) and Nd isotopes to decipher tectonic setting, source rock composition and changes in provenance over time.

2. Geological background

The evolution of the Tarfaya basin has been closely connected with the geological history of the African Craton and the opening of the Atlantic Ocean (Ranke et al., 1982), with development from a rift to a marginal basin. The basin is filled by Mesozoic and Cenozoic continental to shallow marine sediments overlying a basement of Precambrian and/or Paleozoic age. According to Choubert et al. (1966), Auxini (1969) and Dillon and Sougy (1974), Triassic evaporites, redbeds, reddish sandstone, conglomerates and volcanic rocks overlie either metamorphic or folded rock sequences of the Mauritanides or crystalline rocks of the Reguibat Shield (West African Craton). The Early Jurassic marine carbonates transgressed onto the Triassic rift sediments and/or evaporate. Silty sandstone, limestone, dolomitic limestones, and dolomites of Early to Middle Jurassic are overlain by Late Jurassic neritic marly limestone and calcarenites, intercalated with marls, shales and sandstones. A thick deltaic sequence of the Early Cretaceous accumulated during and after a major global Valanginian regression (Vail et al., 1977). According to Ratschiller (1970), the shallow-marine from the Late Cretaceous to Early Eocene unconformably overlies the continental Early Cretaceous formations. The Late Oligocene to Early Miocene basin development shows an erosional hiatus because of the coincidence of a major regression with intensified slumping, canyon incision and an intensification of bottom water circulation (Arthur et al., 1979), with only little continental deposition. Since the Miocene–Pliocene sedimentary deposition started again with clastic sediments unconformably overlying the Late Cretaceous (NE part of the basin), Early Eocene and Oligocene (SW part of the basin). This latest depositional phase coincided with uplift events in the Anti-Atlas (Frizon de Lamotte et al., 2009; Ruiz et al., 2010).

2.1. Potential source areas of sediments surrounding the Tarfaya basin

The Tarfaya basin (Fig. 1) is located at the margin of the western Atlantic and has been filled by siliciclastic sediments originating from the Reguibat Shield and the Mauritanides in the SW (West African Craton, WAC) and from the western Anti-Atlas in the NE of the basin (Michard et al., 2008). The WAC basement exposed in the Reguibat shield consists of rocks with two contrasting

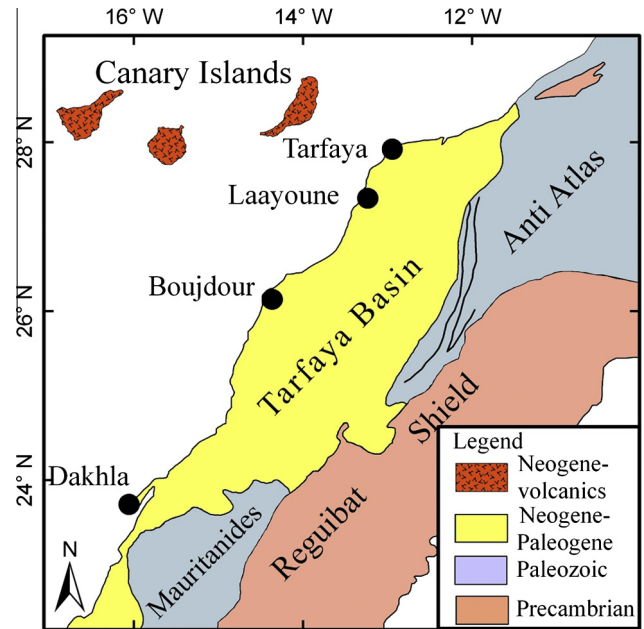


Fig. 1. General map of the study area and possible surrounding source regions (modified after Michard et al., 2008).

deformational ages of the crustal domains, namely a western terrain of Archean age and an eastern terrain of Eburnean age. According to Lahondere et al. (2003), the western Archean terrain is dated at 3.04–2.83 Ga, whereas rocks of the eastern Eburnean terrain are much younger, i.e. 2.12–2.06 Ga (Schofield et al., 2006; Schofield and Gillespie, 2007). According to Frizon de Lamotte et al. (2009) and Ruiz et al. (2010), the western Anti-Atlas consists of sediments that were mainly derived from various Precambrian inliers and/or the West African Craton. These sediments are characterized by a high proportion of fine grained detrital, clay rich sediments intercalated with thin beds of muddy siltstones and shales, quartzites, sandstones, limestones and conglomerates at different stratigraphic levels. This sedimentary cover was uplifted, folded and mildly metamorphosed during the Variscan Orogen (Late Paleozoic) (see Michard, 1976; Soulaïmani et al., 1997; Helg et al., 2004; Michard et al., 2008).

3. Materials and methods

In the present study, a number of sections cropping out in the Sebkhas and along the shoreline from the Early Cretaceous to Miocene–Pliocene (SW and NE parts of the basin) have been systematically logged and investigated, complemented by sections obtained from four newly drilled cores. The location of the sections and drilled cores are shown in Fig. 2 and sample positions within sections are given in Figs. 3a and 3b. Photomicrographs of selected samples are also shown in Fig. 4. The Boukhchebat section of Early Cretaceous, which outcrops in the NE part of the basin, consists of coarse sandstones (in the lower part) and sandstones intercalated with sandy marls and shales. Late Cretaceous sections, which are primarily exposed in the NE part of the basin consists of black shales and sandy marls intercalated with cherts and nodular or bedded limestones. Early Eocene deposits are mainly outcropping in the SW part of the basin and comprise black shales and sandy marls intercalated with cherts and limestones. Oligocene–Early Miocene sandy marls were sampled in the Sebkha Aridal section. Miocene–Pliocene siliciclastic deposits consist of coarser or conglomeratic sandstones, sandstones and together with lumachelle in the lower part of the sections, directly deposited on the

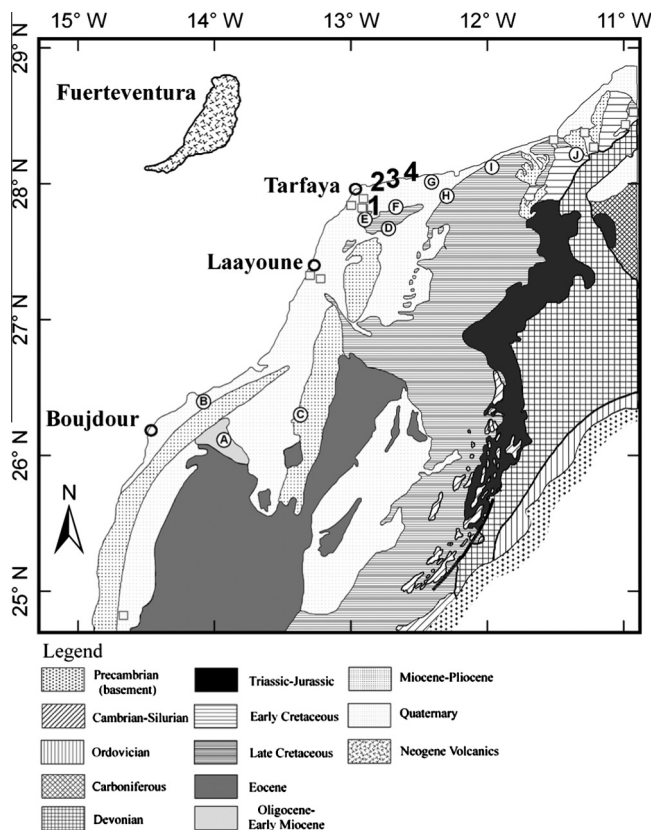


Fig. 2. Geological map of the Tarfaya basin showing the geological formations of Precambrian to Quaternary (Modified after Ranke et al., 1982). Along with, sampled sections, drilled cores positions and recent sediment samples locations. A = Sebkha Aridal, B = Sebkha El Farma, C = Oued El Khatt, D = Sebkha Tah (E), E = Sebkha Tah (W), F = Sebkha Tisfourine, G = Onhym Quarry, H = Akhfennir, I = Amma Fatma, J = Boukhchebat, 1–4 drilled cores (see also Table 1 Appendix A) Square box locations of the recent sediment samples. □

weathered horizon of the Late Cretaceous. The Pleistocene and recent sediment samples were also collected from various Wadis. In total, 109 samples from 10 stratigraphic sections from SW and NE parts of the Tarfaya basin and from four newly drill cores, as well as recent sediment samples from Wadis were selected for trace element analysis. Furthermore, 39 selected samples were also used for Nd–Sr isotope analyses.

The samples were cleaned for geochemical analysis after removing weathered coatings and veined surfaces. These samples were broken into small pieces of about 4 mm in size by a pestle and were then dried, crushed, powered and homogenized.

About 150 mg of each sample were first dissolved carefully in dilute HNO_3 in Teflon vials to dissolve excess carbonates prior to the digestion process of the silicate fraction. In the second step, a mixture of concentrated sub-boiled HNO_3 – HCl – HF (3:1:4) was used for first-step dissolution overnight at 160 °C. After evaporation to near dryness, a pressure bomb step was used for complete dissolution of all silicates including the heavy minerals. Concentrated HNO_3 and HF (1:4) were added and the bombs (Parr bombs) were heated for 4 days at 160 °C. In the final step, perchloric acid was added and then evaporated nearly to dryness. The residue was re-dissolved in dilute HNO_3 (1:4) and made up to a final volume of 50 ml. This analytical work was performed at the Institute of Geosciences, Kiel University, Germany. A total of thirty seven trace elements were analyzed using inductively coupled plasma mass spectrometry (ICP-MS, Agilent 7500cs). Details of sample preparation techniques and calibration strategies are given by Garbe-Schönberg (1993). The accuracy and precision of the method

was monitored with control samples and duplicates and by running USGS international rock standards G-2, BHVO-2 and AC-E. The error of replicate analyses was better than 5% for all analyzed trace elements.

Nd–Sr isotope measurements were carried out on a Multi-Collector ICP-MS (Nu Plasma) at GEOMAR. For isotope analysis, 150 mg powder of each sample was first dissolved in dilute HNO_3 in PFA (perfluoroalkoxy, Savillex TM) vials and carbonate was completely removed before initiation of the digestion process of the silicate fraction. In the second step, samples were completely digested by using a mixture of concentrated HF – HNO_3 – HClO_4 . The separation and purification of Nd and Sr from the totally digested samples followed previously published procedures for Nd (Barrat et al., 1996; Cohen et al., 1988; Le Fèvre and Pin, 2005) and Sr (Bayon et al., 2002; Horwitz et al., 1992). $^{143}\text{Nd}/^{144}\text{Nd}$ ratios were mass-bias-corrected to $^{146}\text{Nd}/^{144}\text{Nd} = 0.7219$ and were then normalized to the accepted value of the JNdi-1 standard of 0.512115 (Tanaka et al., 2000). Repeated measurements of the JNdi-1 standard over a period of several months gave a long-term reproducibility of ± 0.35 (2σ). Procedural Nd blanks were ≤ 25 pg. Measured Sr isotope ratios were interference (^{86}K , ^{87}Rb) and mass bias corrected (using $^{86}\text{Sr}/^{87}\text{Sr} = 0.1194$, Steiger and Jäger, 1977), $^{86}\text{Sr}/^{87}\text{Sr}$ results were normalized to that of NIST NBS987 = 0.710245, which was measured between samples. The 2σ external reproducibility during the measurements for this study was ± 0.00004 . Procedural Sr blanks were less than 0.7 ng.

4. Results

4.1. Trace elements

Trace element compositions of the studied samples from the Early Cretaceous to recent in the Tarfaya basin are given in Table 1 Appendix A. All the analyzed trace element concentrations have been normalized to average Upper Continental Crust (UCC, Taylor and McLennan, 1985; McLennan, 2001). In the spider diagrams (Fig. 5), UCC-normalized trace elements are arranged in order of increasing atomic number. The concentrations of trace elements vary widely and most of the elements have a lower abundance than that of UCC.

4.1.1. Large-ion lithophile elements (LILE, Rb, Cs, Ba, Sr), Th and U

The concentration of LILE in the analyzed samples is variable (Table 1 Appendix A). Most of them are moderately to strongly depleted in LILE (Table 1 Appendix A, Fig. 5) when compared with UCC. The alkali element Rb is highly variable and ranges from 11 to 133 ppm, with Cs varying from 0.88 to 3.0 ppm. The average abundance of Ba (402 ppm) is higher in the Early Cretaceous sandstone samples than in other analyzed samples. The Sr concentration, on average, in shale and marl samples from the Late Cretaceous and Early Eocene is 508 ppm and 402 ppm, respectively, and relevant values in the recent sediments (414 ppm) are higher than those of other rocks in other stratigraphic ages. When Sr is compared with CaO content, we have found that the Sr content in shale and marl samples are highly correlated ($r = 0.91$), but are only weakly correlated in sandstone samples ($r = 0.21$). Hence, this high correlation between Sr and CaO in shale and marl samples indicate their contribution was mainly from sea water/marine carbonate in equal proportion.

The positive correlations between K_2O –Rb ($r = 0.94$), K_2O –Cs ($r = 0.81$) and K–Ba ($r = 0.51$) provide evidence that K-bearing clay minerals (illite, muscovite and biotite) primarily control the abundance of these elements (McLennan et al., 1983; Feng and Kerrich, 1990). All studied samples show high positive correlations between Al_2O_3 –Rb ($r = 0.90$) and Al_2O_3 –Cs ($r = 0.96$) further support-

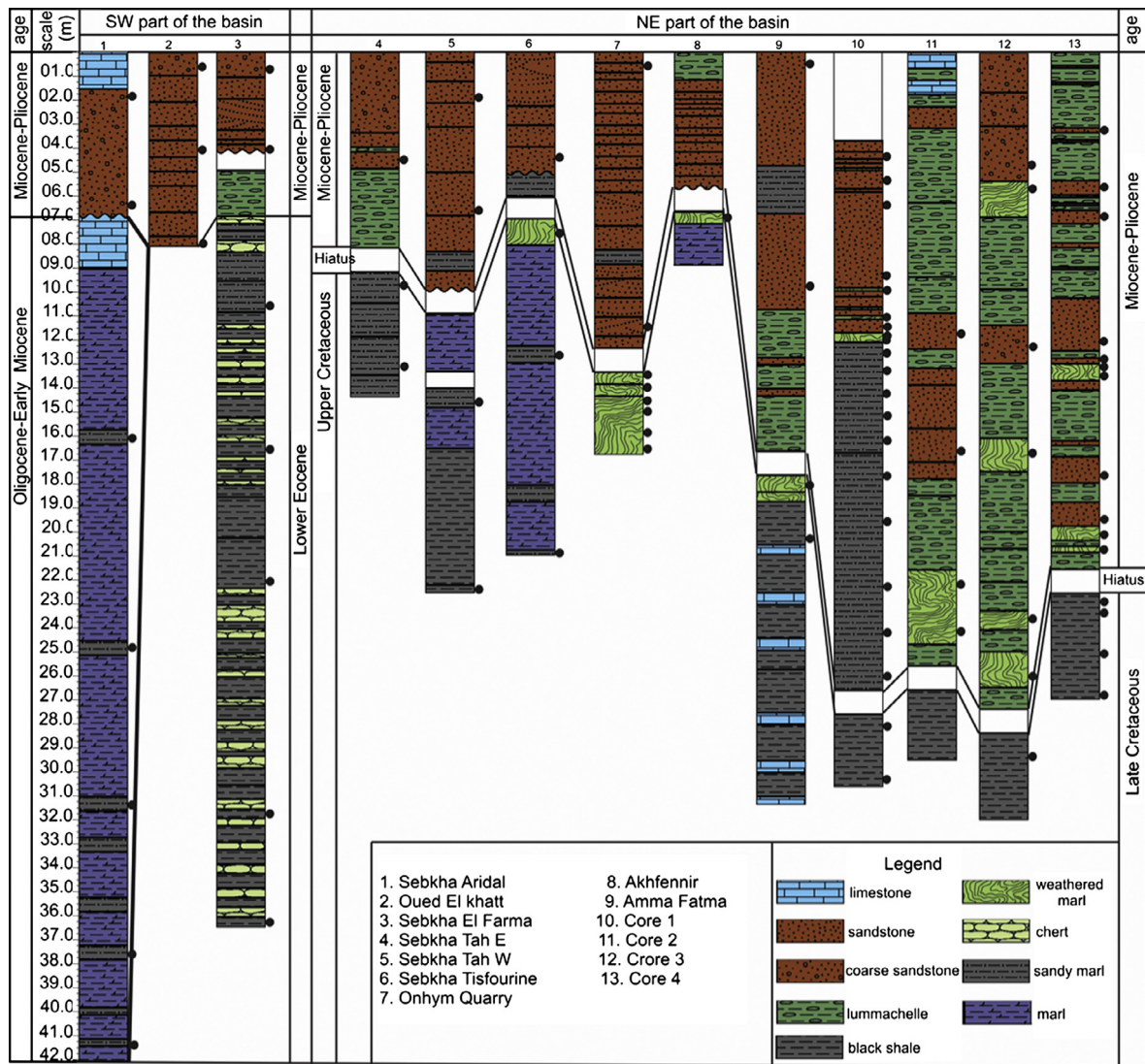


Fig. 3a. Lithologic sections of the Tarfaya basin from Late Cretaceous to Miocene–Pliocene time. Black dots mark sample positions.

ing the idea that the distribution of these elements is possibly controlled by phyllosilicates (Bauluz et al., 2000). However, a weaker and non-significant positive correlation between Al_2O_3 –Ba ($r = 0.39$) implies that other factors may also have controlled the abundance of Ba.

The Th concentration is low when compared with that of UCC. Uranium is highly variable (0.4–28 ppm) and the highest value was found in black shale sample #C1-35 (110 ppm, Table 1 Appendix A). In general, shale and marl samples are enriched in U, but sandstones are depleted as compared with UCC. The Th/U ratios are found to be much lower than UCC in all studied samples (Table 1 Appendix A).

4.1.2. High field strength elements (HFSE, Zr, Hf, Y, Nb and Ta)

HFSE are preferentially partitioned into melts during crystallization and anatexis (Feng and Kerrich, 1990), and as a result, these elements are enriched in felsic rather than mafic rocks. Because of their immobile characteristics, these elements are considered as a good provenance indicator, together with REEs (Taylor and McLennan, 1985).

The average concentration of HFSE is depleted when compared with UCC, except for some elements in a few samples (Table 1

Appendix A, Fig. 5). Zr and Hf are variably concentrated in the diverse stratigraphic ages and are highly enriched in the Oligocene–Early Miocene sandy marls and Miocene–Pliocene (NE part of the basin) sandstone samples. These Oligocene–Early Miocene and Miocene–Pliocene stratigraphic ages show average concentrations of Zr of 253 ppm and 460 ppm and Hf of 5.6 ppm and 9.4 ppm, respectively. The Y abundance is higher in the sandy marls of Miocene–Pliocene stratigraphic age (core 1). The average concentrations of Ta and Nb are higher in the recent sediments at 8.0 ppm and 0.56 ppm, respectively.

The Zr/Hf ratios in all the analyzed sediments (Table 1 Appendix A) range from 24 to 51 (average 40), excluding two samples having higher ratios 70 (sample #16-10) and 82 (sample # C1-09), implies that these elements are controlled by the abundance of zircons. The average Zr/Hf ratios in studied rocks of different stratigraphic ages are higher when compared with UCC (32.8, Taylor and McLennan, 1985), possibly indicating that they are the result of sediment recycling during transport.

4.1.3. Transition trace elements (TTE, Cr, V, Co, Ni and Sc)

The transition metals Cr, V, Co, Ni and Sc generally behave similarly as highly compatible elements during magmatic fraction-

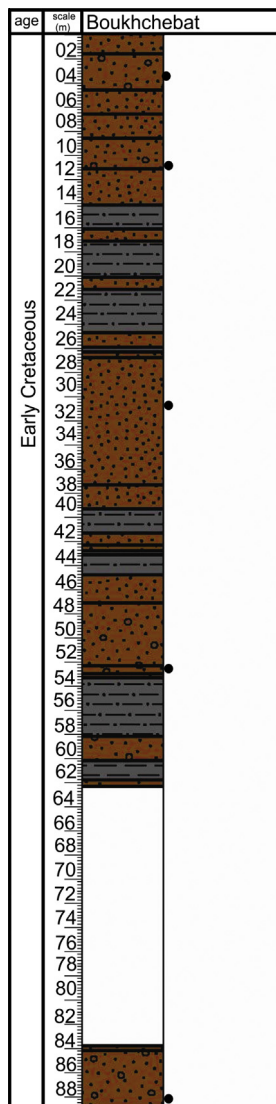


Fig. 3b. Lithologic sections of the Tarfaya basin from Early Cretaceous time. Black dots mark sample positions. Legend is same as in Fig. 3a.

ation processes, being enriched in mafic to ultramafic rocks. However, during weathering, they might be mutually fractionated (Feng and Kerrich, 1990).

The shale samples from the Late Cretaceous and Early Eocene (Table 1 Appendix A, Fig. 5) are more concentrated in Cr, V and Ni, being higher than in UCC. This may be attributable to enrichment together with the organic matter and the formation of secondary minerals. Co and Sc show variable abundance and higher values are found in recent sediments.

The most significant correlations exist between K_2O -Sc ($r = 0.76$), K_2O -Co ($r = 0.49$), Al_2O_3 -Sc ($r = 0.94$) and Al_2O_3 -Co ($r = 0.81$) suggesting that they were controlled by weathering and concentrated in the phyllosilicates. Cr, V and Ni are more scattered and less correlated with K_2O and Al_2O_3 indicating that variable factors controlled the distribution of these elements. Furthermore, the Cr, V and Ni elemental concentration is higher in the shale and marl samples, especially in black shales, indicating that their higher concentration is attributable to organic matter, despite that measurements of the organic content were not carried out. These elements were evidently enriched under anoxic conditions. These anoxic events in the Tarfaya basin during Late Cretaceous were discussed by Kuhnt et al. (1997, 2005, 2009).

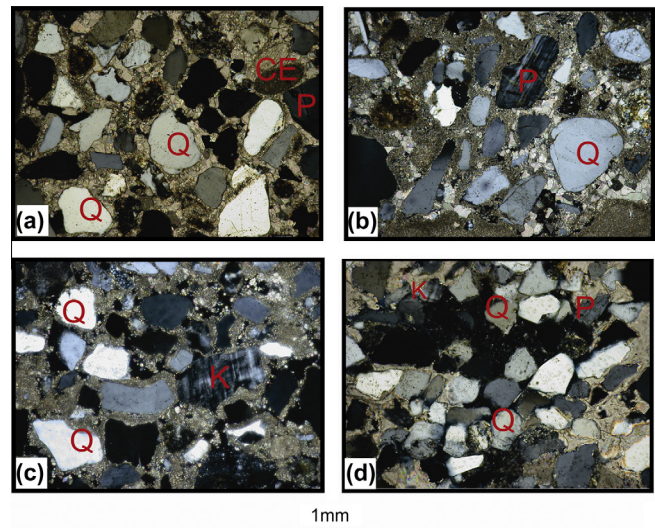


Fig. 4. Photomicrographs of the Tarfaya basin sandstones: a = Amma Fatma Khatt (Miocene–Pliocene NE part of the basin), b&c = Sebkhia El Farma (Miocene–Pliocene SW part of the basin) and d = Boukhchebat (Early Cretaceous). Q = Quartz, P = Plagioclase, K = K-feldspar, CE = Carbonate extrabasinal alteration.

4.2. Rare earth elements (REE)

The concentration of REEs is given in Table 2 Appendix A and chondrite-normalized REE patterns are shown in Fig. 6 and compared with the Post Archean Australian Shale-normalized patterns (PAAS; Taylor and McLennan, 1985). Despite variable concentrations, their distribution patterns are similar to PAAS. Moreover, we found that these elements are less abundant than in UCC most likely due to their high carbonate contents (Taylor and McLennan, 1985). In general, chondrite-normalized REE patterns for studied samples appear similar (Fig. 6), characterized by high LREE/HREE ratios, almost flat HREE patterns and pronounced but variable Eu anomalies. Their variation in absolute concentration reflects mostly the carbonate contents and the variation in the grain size and also clearly shows that any seawater fractionation is absent supporting the fully detrital (siliciclastic) origin of the trace elements. However, a slight variation is present in the distribution of HREE (Dy to Lu).

The analyzed samples (Table 2 Appendix A) have Eu/Eu^* values in the range of 0.60–0.92. The La/Sm Gd/Yb and La/Yb ratios range from 4.2 to 8.6, 1.4 to 3.2 and 8.1 to 18.2, respectively. The Y/Ho ratios vary from 1.8 to 3.3 with an average of 2.4, which is close to that of UCC. However, most of the shale and marl samples show a slightly higher ratio of Y/Ho than is found in UCC, potentially indicating a small contribution of these elements from refractory marine carbonates (Bau et al., 1995; Bau, 1999).

In addition, a weak positive correlation between Zr-HREE ($r = 0.42$) indicates that HREE fractionation is only in part controlled by the occurrence of zircon. This is further supported by a weak negative correlation of $Zr-(Gd/Yb)_N$ ($r = -0.41$) (where the subscript 'N' refers to chondrite-normalized abundances) correlation. Zircon is typically enriched in HREE resulting in values <1 for $(Gd/Yb)_N$. This is in contrast to the average HREE distribution in UCC rocks having $(Gd/Yb)_N > 1$. Both LREE and HREE show a high positive correlation with $LREE-Al_2O_3$ ($r = 0.88$) and $HREE-Al_2O_3$ ($r = 0.80$) and with $LREE-TiO_2$ ($r = 0.90$) and $HREE-TiO_2$ ($r = 0.87$) but no correlation with $LREE-P_2O_5$ ($r = 0.12$) and $HREE-P_2O_5$ ($r = 0.26$). This indicates the variable influence of aluminosilicates such as phyllosilicates and zircon, but no control of phosphate minerals, which are highly enriched in REEs.

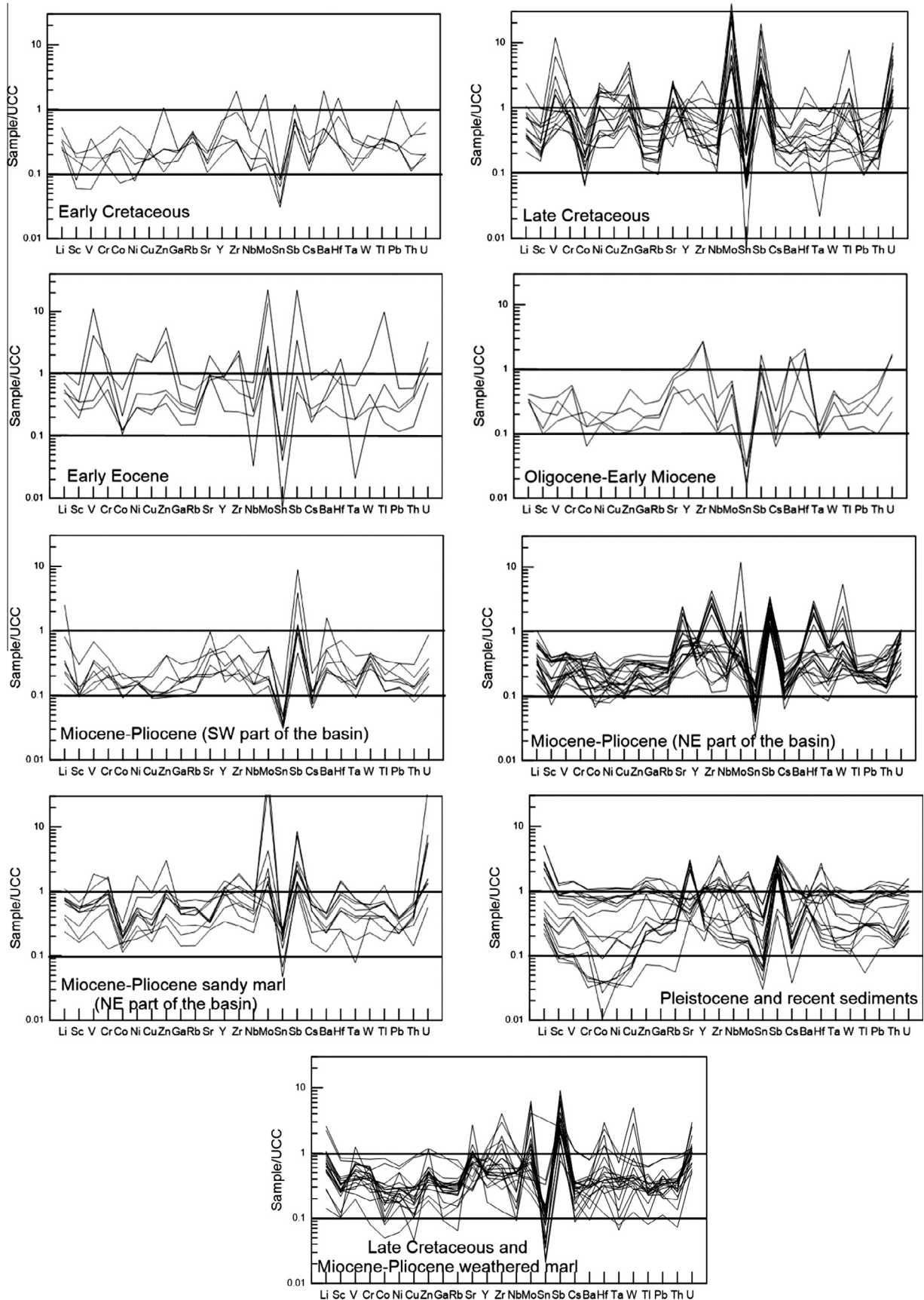


Fig. 5. Trace element concentrations of the studied samples from Early Cretaceous to recent in the Tarfaya basin normalized to the composition of average Upper Continental Crust (UCC; Taylor and McLennan, 1985; McLennan, 2001).

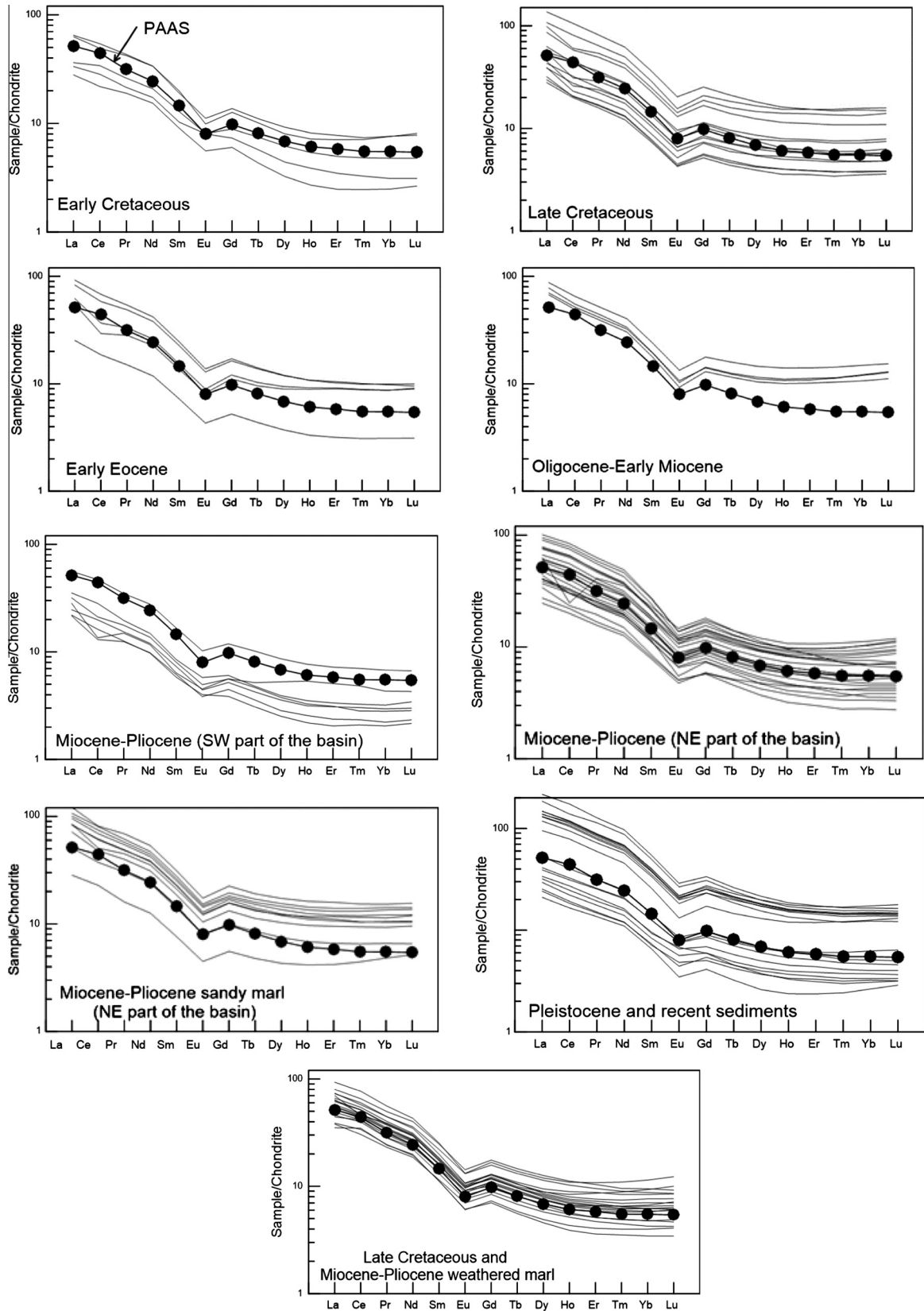


Fig. 6. Chondrite normalized REE patterns of the studied samples from Early Cretaceous to recent in the Tarfaya basin.

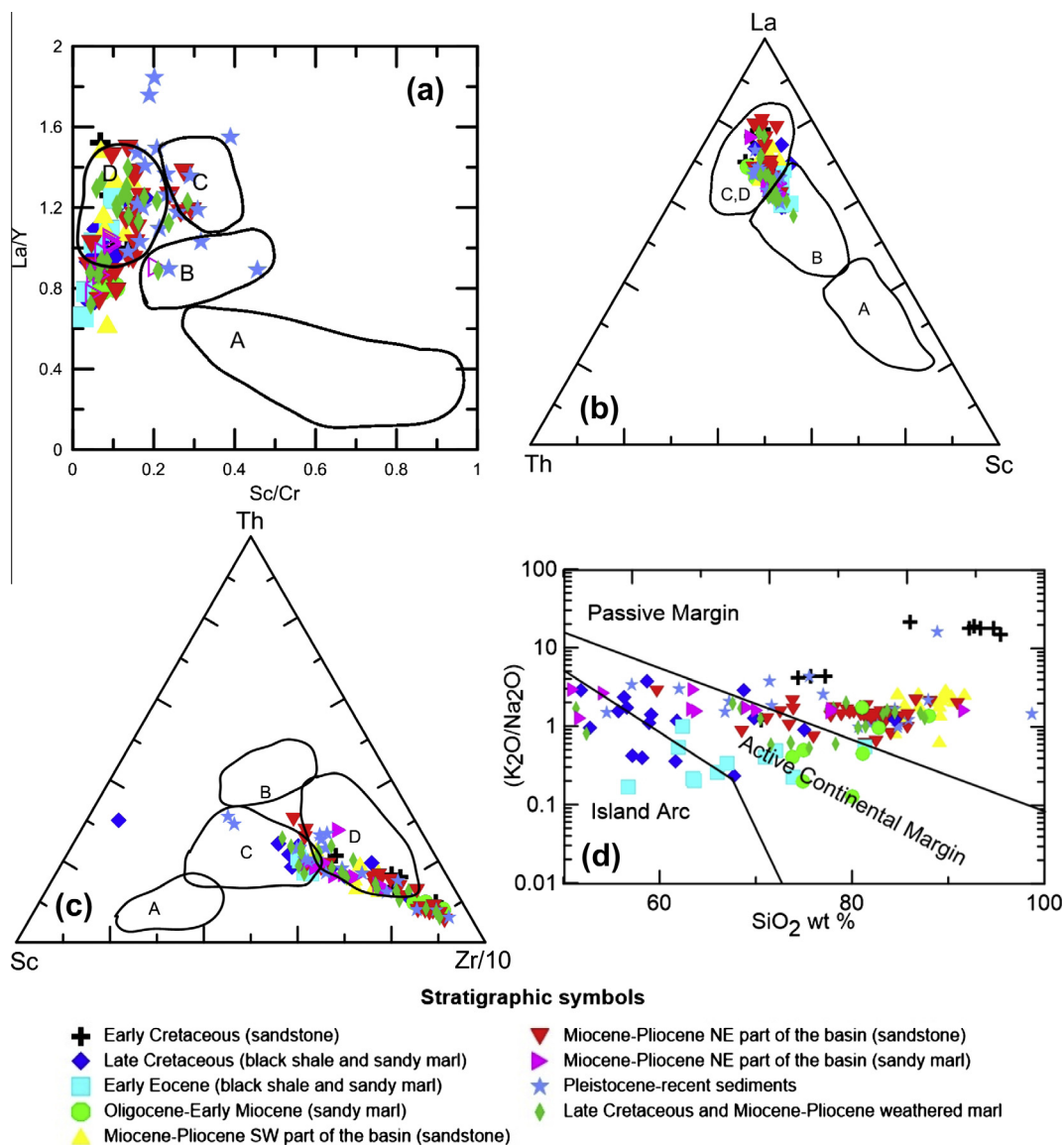


Fig. 7. Plots of the major and trace element compositions from the Tarfaya basin on the tectonic-setting discrimination diagrams of Bhatia (1983): a–c; Roser and Korsch (1986): d. a: Oceanic Island Arc, b: Continental Island Arc, c: Active Continental Margin, d: Passive Margin. Figure d used as a reference.

4.3. Sm–Nd isotopes

The data for the $^{143}\text{Nd}/^{144}\text{Nd}$ isotopic composition of 39 samples are given in Table 3 Appendix A and the calculated provenance ages (T_{DM}) against the various stratigraphic ages are illustrated in Fig. 11 (note that the carbonates were removed prior to the preparation for Nd and Sr isotope measurements). Although, Sm (0.87 to 8.3 ppm) and Nd (4.6 to 45 ppm) values are somewhat lower than UCC and PAAS, the $^{147}\text{Sm}/^{144}\text{Nd}$ ratios in the sediments (0.1081–0.1244) are equivalent or slightly higher than typical terrigenous sediments (0.105–0.115; Taylor and McLennan, 1985).

A total of four analyzed sandstone samples from the Boukhchebat section of the Early Cretaceous show ranges in $\epsilon_{\text{Nd}}(0)$ values from -15.7 to -19.2 and have an average value of -17.1 , $^{147}\text{Sm}/^{144}\text{Nd}$ ratios of 0.1080, T_{CHUR} ages of 2.0 Ga, T_{DM} ages range from 2.0 to 2.2 Ga.

Eight shale and marl samples of the Late Cretaceous exhibit $\epsilon_{\text{Nd}}(0)$ values in the range between -14.1 and -15.0 (average 14.6) and similar provenance (T_{DM}) ages (1.8–1.9, average 1.8 Ga). Further, three samples of the Early Eocene also have similar $\epsilon_{\text{Nd}}(0)$ values in the range -14.4 to -14.7 (average -14.3) and,

hence, have model ages (average 1.8 Ga) equivalent to those from the Late Cretaceous sediments.

Because of their similarity, the Nd isotope data of Oligocene–Early Miocene (lower Part) and Miocene–Pliocene (upper part) in the Sebkhya Aridal section are discussed together. Two sandy marl samples from the lower part of the section (Oligocene–Late Miocene) and one sandstone sample from the upper part of this section (Miocene–Pliocene) yielded the most negative $\epsilon_{\text{Nd}}(0)$ values ranging from -23.1 to -25.6 with an average of -24.2 . These samples have $^{147}\text{Sm}/^{144}\text{Nd}$ ratios ranging from 0.108 to 0.117 (average = 0.113). The T_{DM} ages calculated from these samples are the oldest among all the studied samples, ranging from 2.5 to 2.6 Ga (average 2.5 Ga).

Sandstone samples of the Miocene–Pliocene from both parts of the Tarfaya basin show a range of $\epsilon_{\text{Nd}}(0)$ from -12.1 to -13.0 (average -12.6) in the SW part and -12.6 to -17.6 (average -14.8) in the NE part of the basin. However, the average T_{DM} ages at nearly 1.8 Ga are similar in both parts of the basin. One sample from drill core-4 (sample #C4-03) yielded a more positive $\epsilon_{\text{Nd}}(0)$ value of -9.8 and, hence, a younger T_{DM} age of 1.5 Ga, which is possibly due to a contribution from other younger source areas.

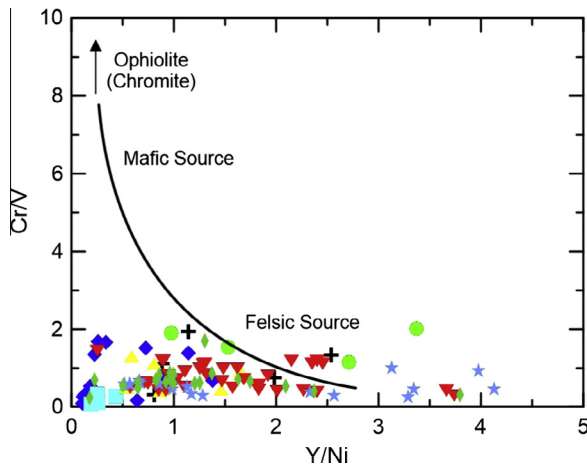


Fig. 8. Analyzing the provenance by using relations of Cr/V versus Y/Ni (after Hiscott, 1984). Curve model between granite and ultramafic end members. Ultramafic rocks have very low Y/Ni and high Cr/V ratios. Arrow indicates the direction of the mafic-ultramafic source end-end members. Legend is same as in Fig. 7.

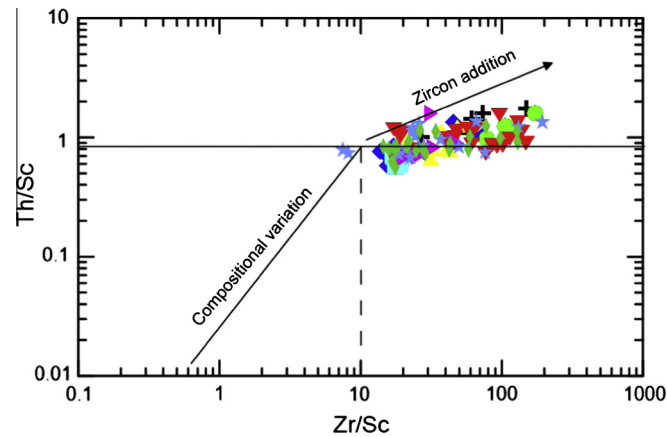


Fig. 9. Th/Sc versus Zr/Sc Plot (after McLennan et al., 1993). Explanation for both the compositional variation trend line and the zircon addition trend line can be found in the text. Legend is same as in Fig. 7.

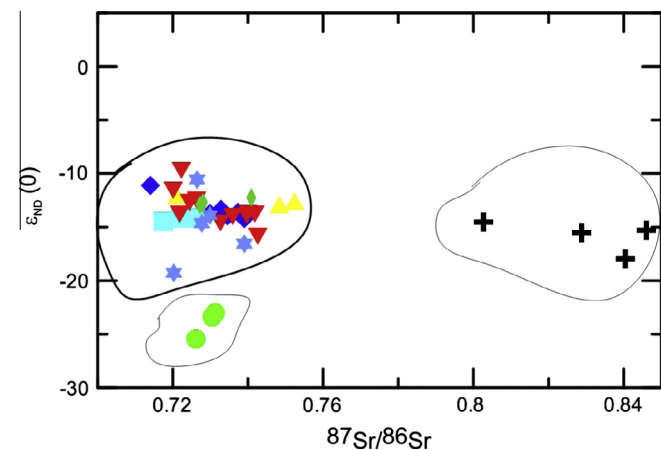


Fig. 10. $\epsilon_{Nd}(0)$ versus $^{87}Sr/^{86}Sr$ plots for studied samples from the Tarfaya basin. Legend is same as in Fig. 7.

Four recent sand samples of recently deposited sediments from Wadis provide variable $\epsilon_{Nd}(0)$ values ranging from -13.9 to -19.3 (average -16.3). The T_{DM} ages consequently range from 1.7 to

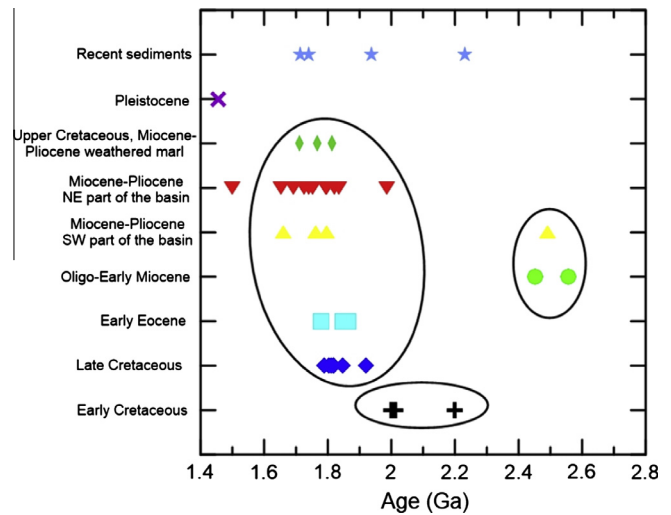


Fig. 11. Provenance ages against stratigraphic age plots of the Tarfaya basin. Legend is same as in Fig. 7.

2.2 Ga. The southernmost sample (# 14-01) exhibits the oldest T_{DM} age (2.2) among the four recent sediment samples. In addition, one Pleistocene sand sample has an $\epsilon_{Nd}(0)$ value of -10.6 , which is again more positive compared with the other sand samples and yields a younger provenance age of 1.5 Ga.

In order to determine the direct effect of weathering processes on the obtained Nd-isotope compositions, three samples, one Late Cretaceous weathered marl sample from the Onhym quarry and two Miocene–Pliocene weathered marl samples from drilled cores (Table 3 Appendix A), have been analyzed. The weathered marls exhibit $\epsilon_{Nd}(0)$ values ranging from -13.0 to -13.7 (average -13.4), a similar $^{147}Sm/^{144}Nd$ ratio (0.20), T_{CHUR} ages from 1.3 to 1.4 Ga (1.4 Ga on average) and T_{DM} ages varying from 1.7 to 1.8 Ga (1.8 Ga on average). The T_{CHUR} and T_{DM} ages obtained from weathered marls are compatible with the Late Cretaceous and Miocene–Pliocene provenance ages implying that weathering process did not significantly alter the Nd isotope compositions and hence the model ages.

4.4. Rb–Sr isotopes

Thirty nine samples from various stratigraphic ages were also analyzed for their radiogenic Sr isotope composition (Table 4 Appendix A). The Early Cretaceous sandstone samples show higher $^{86}Sr/^{87}Sr$ values, ranging from 0.8027 to 0.8461, than all other younger sediments. During the Late Cretaceous more variable, but less radiogenic $^{86}Sr/^{87}Sr$ ratios have been found including those of the Late Cretaceous (average 0.7285), Early Eocene (0.7268), Oligocene–Early Miocene and Miocene–Pliocene (0.7309, Sebkhah Aridal section), Miocene–Pliocene SW part of the basin (0.7369), NE part of the basin (0.0.7316), Pleistocene and recent sediments (0.7289) and weathered marls (0.7327). The calculated $^{86}Sr/^{87}Sr$ compositions at stratigraphic age (I_{Sr}) are also highly variable ranging from 0.7976 to 0.8398 during the Late Cretaceous and from 0.7140 to 0.7523 between the Late Cretaceous and the present.

4.5. Nd–Sr isotope fractionation

According to McLennan et al. (1993) $f^{Sm/Nd}$ is the fractional deviation of the $^{147}Sm/^{144}Nd$ from that in chondritic meteorites ($f^{Sm/Nd} = (^{147}Sm/^{144}Nd)_{sample} / (^{147}Sm/^{144}Nd)_{chondrite-1}$) and monitors the general level of differentiation. The studied sediments of the Tarfaya basin show a narrow range of $f^{Sm/Nd}$ from

–0.35 to –0.45 (Table 3 Appendix A). A poor correlation also exists between the $^{144}\text{Sm}/^{147}\text{Nd}$ ratios and $\varepsilon_{\text{Nd}}(0)$ values ($r = 0.41$). This indicates that no resetting of Sm–Nd compositions occurred during sedimentary and post-sedimentary processes (McLennan et al., 1993; Bock et al., 1994; McDaniel et al., 1994; Xie et al., 2012). On the other hand, the $^{87}\text{Rb}/^{86}\text{Sr}$ ratios of the sediments studied show a large variation range from 0.010 to 3.65, possibly resulting from grain size sorting and Rb–Sr redistribution during post-sedimentary processes (Xie et al., 2012). Therefore the provenance reconstructions based on the Sm–Nd isotope system is considered more robust and thus used here to place constraints on the provenance of the Tarfaya basin detrital sediments.

5. Discussion

5.1. Tectonic setting

The major and trace element geochemical compositions of sedimentary rocks has been extensively used to discriminate tectonic settings of sedimentary basins (Bhatia, 1983, 1984, 1985; Roser and Korsch, 1986, 1988; McLennan and Taylor, 1991). Further, Bhatia and Crook (1986) have also used immobile trace element compositions of greywackes to discriminate different tectonic settings. However, these criteria must be used with caution, as sometimes sediments are transported from their tectonic setting of origin into a sedimentary basin in a different tectonic environment (McLennan et al., 1990; Armstrong-Altrin and Verma, 2005).

The La/Y versus Sc/Cr binary diagram (Fig. 7a) suggests a passive continental margin setting for the studied samples, as most of the studied samples plot inside the passive margin field or clustering near to the field (Bhatia and Crook, 1986). In the La–Th–Sc triangular diagram (Fig. 7b) samples plotted in the passive margin field, demonstrate a passive continental margin depositional setting. Furthermore, the Th–Sc–Zr/10 diagram (Fig. 7c) of tectonic setting discrimination, most of the data plot inside the passive margin field or near to the field except few exceptions, also demonstrates a passive continental margin setting. In addition, major element compositions of Early Cretaceous, Miocene–Pliocene sandstones and recent sands, according to the binary tectonic discrimination scheme of Roser and Korsch (1986), also suggest a passive marginal tectonic setting (Fig. 7d, used as a reference after Ali et al., manuscript in review). However, plots of shale and marl samples from the Late Cretaceous, Early Eocene and Oligocene–Early Miocene are more scattered due to lower SiO_2 and high Na_2O contents in these more fine grained sediments and are thus less representative of the tectonic setting of the basin. Hence, trace element compositions were found more useful for discriminating the tectonic setting of the Tarfaya basin sediments than major element compositions. Finally, our results indicate that the Tarfaya basin sediments were deposited in a passive margin tectonic setting since Cretaceous and are in agreement with the tectonic history of the basin (Ranke et al., 1982; Michard et al., 2008).

5.2. Source rock composition

The abundance of Cr and Ni in clastic sediments can be considered a proxy in provenance studies. A high content of Cr and Ni is predominantly found in sediments derived from ultramafic rocks, whereas a low concentration of Cr and Ni indicates a felsic provenance (Wrafter and Graham, 1989; Garver et al., 1996; Armstrong-Altrin et al., 2004). Garver et al. (1996) have shown that elevated Cr and Ni abundances ($\text{Cr} > 150$ ppm and $\text{Ni} > 100$ ppm), low Cr/Ni ratios (1.3–1.5) and a high correlation coefficient between these two elements ($r = 0.90$) are indicative of ultramafic rocks in the source region. The Cr (3.3–149.1) and Ni (1.4–106.8) concentrations

(Table 1 Appendix A) in most of the studied samples are relatively low, with a less significant correlation coefficient ($r = 0.60$) and variable Cr/Ni ratios (0.5–6.6). These low Cr and Ni concentrations in the studied samples may be not showing clear indication of source rocks composition due to carbonate dilution effects. However, high and variable Cr/Ni ratios and less significant correlation between Cr and Ni in the studied samples do not indicate any signature of mafic or ultramafic rocks in the source region. Furthermore, a binary diagram (Fig. 8) of Cr/V versus Y/Ni ratios has also been used to discriminate the source area (Hiscott, 1984; McLennan et al., 1993). The Cr/V ratios serve as index of the enrichment of Cr over the other ferromagnesian trace elements, whereas Y/Ni monitors the general level of ferromagnesian trace elements (Ni) compared with a proxy for HREE (Y). The mafic to ultramafic sources tend to have higher Cr/V and lower Y/Ni ratios. The samples in the present study have an extremely low Cr/V ratio and a variable abundance of Y/Ni exhibiting a predominantly felsic lithology of the source area. Hence, these low Cr/V and variable Y/Ni ratios preclude any presence of the ophiolitic component in the source regions.

The ratios between relatively immobile trace elements such as La/Sc, Th/Sc, Cr/Th and Th/Co are considered suitable indicators of source rock provenance (Taylor and McLennan, 1985; Cullers, 1994, 2000; Cullers and Podkovyrov, 2000; Wronkiewicz and Condie, 1990). In the present study, these ratios are compared with those of sediments derived from felsic and mafic rocks and also with UCC (Table 5 Appendix A). The comparisons show that the majority of our data are within the range of felsic source rocks and lower than UCC. According to Armstrong-Altrin et al. (2004), La/Sc and Th/Sc ratios of sediments derived from felsic rocks are always higher than those of sediments derived from mafic rocks. Although some of the samples have slightly lower values of Th/Sc ratios. However, Th/Sc ratios are still much higher than those of mafic rocks and also demonstrate a felsic source. Furthermore, Most of the studied samples have Cr/Th ratios close to those of UCC ($\text{Cr/Th} = 7.76$, McLennan et al., 2006). The Th/Co ratios of the studied samples also lie within the range of felsic source and are very close to those of UCC (Table 5 Appendix A).

The REE patterns of the source rocks are preserved in clastic sediments (Taylor and McLennan, 1985). Felsic rocks contain higher LREE/HREE ratios and negative Eu anomalies, whereas mafic rocks generally contain lower LREE/HREE ratios with little or no Eu anomalies (Cullers and Graf, 1983; Cullers, 1994). Hence, the REE patterns help to distinguish between felsic and mafic source rock lithologies of clastic sediments. The studied samples of the Tarfaya basin have high LREE/HREE ratios and moderately negative Eu anomalies. The chondrite-normalized samples show REE patterns similar to that of PAAS, with LREE enrichment, an almost flat HREE and negative Eu anomalies. This also supports generally felsic source rocks of the Tarfaya basin sediments.

The Th/Sc ratios were used as an indicator of chemical differentiation and, hence, to infer compositional heterogeneity of the sources (Cox et al., 1995; Hassan et al., 1999). And, The Zr/Sc ratios were used as an index of sediment recycling in the source region (McLennan et al., 1993). Further, Th/Sc ratios higher than 0.8, if coupled with higher values of Zr/Sc, probably indicate input from mature and/or recycled sources. All the studied samples, when plotted into the Th/Sc versus Zr/Sc binary diagram (Fig. 9) show a positive slope and display higher values of both ratios. The Th/Sc ratios have a narrow range (Table 1 Appendix A), whereas the Zr/Sc ratios exhibit a wide range. A particular trend is shown by Zr/Sc ratios which indicate sediment sorting in the source region. Hence, from the Th/Sc versus Zr/Sc ratios, we identify that the source areas have undergone recycling during sediment transport, together with an increasing abundance of zircons.

In summary, the ratios of La/Sc, Th/Sc, Cr/Th, Th/Co and the REE distribution patterns including Eu/Eu* of the Tarfaya basin siliciclastic sediments indicate that they were derived from felsic source rocks and were neither significantly affected by alteration during transport and cementation nor by dissolution of plagioclase in the case of Eu/Eu* (Cullers (1994, 2000), Cullers and Podkovyrov (2000) and Cullers et al., (1988); see also Table 5 Appendix A). This is strongly supported by the internal consistency of our results and their agreement with those obtained on petrography, heavy minerals and mineral chemistry on a subset of the samples of this study (Ali et al., in press). In addition, the Zr/Sc distribution pattern and Zr/Hf ratios are indicating recycling of sediments in the source area. The Nd and Sr isotopic results are discussed in the next section in order to determine whether the studied sediments originated from a single source or whether mixed provenances were involved from the Early Cretaceous to recent times.

5.3. Provenance of the Tarfaya basin sediments

The analyzed samples of the Tarfaya basin of Early Cretaceous to recent show a range of $\epsilon_{Nd}(0)$ values (Table 3 Appendix A). A clear difference exists in the $\epsilon_{Nd}(0)$ values between the Early Cretaceous and the younger stratigraphic ages and the most negative values occurred in the southernmost Sebkhia Aridal section (Table 3 Appendix A). Hence, the calculated depleted mantle model ages (T_{DM}) of these sediments show significant variations in provenance ages as a function of variation in the source area. Previous findings indicated that during the Early Cretaceous, sediments originated from the WAC and that the contribution of sediments from the western Anti-Atlas to the Tarfaya basin only started during the Late Cretaceous (Frizon de Lamotte et al., 2009; Ruiz et al., 2010; Sehart et al., 2011).

The Nd and Sr isotopic compositions of the studied samples are compared in Fig. 10 and reveal three distinct groups. The first group consists of the samples from the Early Cretaceous sediments, characterized by $T_{DM} = 2.0$ to 2.2 Ga provenance age and by higher Sr-isotopic ratios (average 0.8250). These higher Sr isotope ratios that are not reflected by any differences in the Nd isotope results are clearly attributable to fractionation during transport despite that we have not carried out dedicated grain size analyses. These Sr isotope data are thus not included in the interpretations of sediments provenance. The second group comprises the Late Cretaceous, Early Eocene and Miocene–Pliocene samples, characterized by $T_{DM} = 1.7$ –1.9 Ga provenance ages and by variable Sr-isotopic ratios in the range from 0.7140 to 0.7523. In contrast, the third group, which consists of sediments of the Oligocene–Early Miocene (Sebkhia Aridal section in southernmost section SW part of the basin) is characterized by older provenance ages ($T_{DM} = 2.5$ –2.6 Ga). However, Sr-isotopic ratios are similar to those of the second group. The recent sediment samples show an affinity with these distinct groups. The southernmost sample corresponds to the Early Cretaceous (first group), whereas the other three recent sediment samples are similar to the second group. These different clusters suggest that the sediments originated from distinct source areas over time, which will be discussed below.

5.3.1. Modern sediments provenance

One can directly constrain provenance from modern sediment data providing that no change in the isotopic composition of the source area occurred as a consequence of unroofing processes (Mearns et al., 1989). Four modern river-transported sediment samples, which originated from the Reguibat Shield and the western Anti-Atlas, have been used for this purpose. One sand sample (sample # 14-01) has a provenance age of 2.2 Ga and contains sediments that are derived from the Eburnean terrain (Reguibat Shield), have an age similar to the provenance ages

(2.12–2.06 Ga) obtained by Schofield et al. (2006) and Schofield and Gillespie (2007). This indicates that no change has occurred in the overall isotopic composition of the Reguibat Shield source areas between the Late Cretaceous until the present day because of unroofing processes in the Eburnean terrain. The western Anti-Atlas sediments, deposited during the Paleozoic, were derived from the Precambrian inliers and/or the WAC (Frizon de Lamotte et al., 2009; Ruiz et al., 2010; Michard et al., 2008). There is no isotopic data available from these sedimentary covers. However, in our investigations, two recent sand samples whose detrital sediments are derived from the western Anti-Atlas suggest a provenance age (1.7 Ga) for the western Anti-Atlas source area. Finally, a fourth sample whose sediments were possibly derived from both the Reguibat Shield and the western Anti-Atlas source areas suggest a 1.9 Ga provenance age. The mixed provenance ages of young sediments of the Atlantic Ocean were also found in the range from 1.7 to 1.9 Ga by Cole et al. (2009) and Meyer et al. (2011).

5.3.2. Early Cretaceous sediments provenance

The Early Cretaceous sandstones (Boukhchebat section) have $\epsilon_{Nd}(0)$ values similar to the recent ones. The calculated provenance ages (2.0–2.2 Ga) (Fig. 11) in the Boukhchebat section are comparable with the Eburnean terrain indicating that the source is in the northern part of the Reguibat Shield. Sehart et al. (2011) also indicate that the Reguibat Shield was the main source for the Early Cretaceous sediment based on zircon (U–Th–Sm)/He dating (ZHe). Furthermore, the homogeneously negative Nd isotope values and similar Sm/Nd ratios indicate their passive margin depositional tectonic setting, old provenance and long sedimentary recycling (Zhang et al., 2007).

5.3.3. Late Cretaceous to Miocene–Pliocene sediments provenance

The Late Cretaceous, Early Eocene and Miocene–Pliocene sandstone samples (from both the SW and NE parts of the Tarfaya basin) show more positive $\epsilon_{Nd}(0)$ values with a narrow range of provenance ages from 1.7 to 1.9 Ga (average 1.8 Ga) (Table 3 Appendix A, Fig. 11). This indicates that changes in the source of the detrital sediments in the Tarfaya basin for the first time occurred during the Late Cretaceous. This shift may be attributable to the sediments starting to originate from the western Anti-Atlas as a consequence of its uplifting and erosion (Frizon de Lamotte et al., 2009; Ruiz et al., 2010). Previous findings also indicate that the contribution of sediments from the western Anti-Atlas to the Tarfaya basin only started during the Late Cretaceous (Sehart et al., 2011).

Further, three samples from the Sebkhia Aridal section (south most section in the present study) of the Tarfaya basin reflecting Oligocene to Miocene–Pliocene stratigraphic ages show the most negative $\epsilon_{Nd}(0)$ values and hence the oldest provenance ages ($T_{DM} = 2.5$ Ga). These provenance ages are higher than Eburnean (2.12–2.06 Ga) and lower than the Archean terrain (3.04–2.83 Ga) indicating that these provenance ages are a result mixing of detritus from both of these terrains.

6. Conclusions

The geochemical and Nd–Sr isotopic analyses of the sediments from the Early Cretaceous to recent times indicate that the detrital fraction of the Tarfaya basin sediments were deposited in a passive margin tectonic setting, the sediments of which are derived from the heterogeneous source areas of felsic composition. These source areas are in the Eburnean and Archean terrain (Reguibat Shield) along with the Mauritanides and the western Anti-Atlas.

The La/Y versus Sc/Cr, La–Th–Sc and La–Th–Zr/10 diagrams together demonstrate that Tarfaya basin sediments deposited in a

passive margin tectonic setting from Early Cretaceous to recent times. Furthermore, Trace element compositions of more fine sediments better explain tectonic setting of the Tarfaya basin than that of major element compositions.

The La/Sc, Th/Sc, Cr/Th and Th/Co ratios of the Tarfaya basin sediments indicate that these sediments were derived from source rocks of felsic composition. In addition, similarity of REE patterns to that of PAAS, a light rare earth elements (LREE) enrichment, flat heavy rare earth elements (HREE) and negative Eu anomalies support the felsic source for the Tarfaya basin sediments. Moreover, a binary plot of Th/Sc and Zr/Sc as well as Zr/Hf ratios show considerable enrichment of zircon, a finding that indicates recycling of sediments during transport.

The uniform Sm/Nd ratios of sandstone, shale and marl samples from the Early Cretaceous to recent in the Tarfaya basin show that no noticeable fractionation occurred during deposition or diagenesis and, hence, the lack of any modification of the original Nd isotopic compositions.

Further, the Nd isotopic results indicate that the Early Cretaceous sediments were exclusively derived from the Eburnean terrain of the Reguibat Shield. Since the Late Cretaceous, the sediments show mixed contributions from the Reguibat Shield, Mauritanides and the western Anti-Atlas. The supply of the sediments from the western Anti-Atlas has been associated with the tectonic activity in the Anti-Atlas. Finally, the southernmost Sebkhā Aridal section shows predominance of the Archean terrain (Reguibat Shield).

Acknowledgements

We thank RWE Dea for funding this project. We also thank ONHYM for supporting, organizing and accompanying the field campaign in March–April, 2009 and drilling in September–December, 2009. Jutta Heinze and Claudia Teschner are thanked for their help in the laboratory at GEOMAR.

Appendix A. Supplementary material

Supplementary data associated with this article can be found, in the online version, at <http://dx.doi.org/10.1016/j.jafrearsci.2013.11.010>.

References

- Ali, S., Statterger, K., Kuhnt W., Kluth O., Jabour H., Petrography and geochemistry of Cretaceous to Quaternary siliciclastic rocks in the Tarfaya Atlantic marginal basin, SW Morocco: implications for tectonic settings, weathering and provenance. *Int. J. Earth Sci.* 2013 <http://dx.doi.org/10.1007/s00531-013-0965-6>.
- Armstrong-Altrin, J.S., Lee, Y.I., Verma, S.P., Ramasamy, S., 2004. Geochemistry of sandstones from the Upper Miocene Kudankulam Formation, southern India: Implications for provenance, weathering and tectonic setting. *J. Sediment. Res.* 74 (2), 285–297.
- Armstrong-Altrin, Verma, S.P., 2005. Critical evaluation of six tectonic setting discrimination diagrams using geochemical data of Neogene sediments from known tectonic settings. *Sediment. Geol.* 177 (1–2), 115–129.
- Arthur, M.A., von Rad, U., Cornford, C., McCoy, F.C., Sarnthein, M., 1979. Evolution and sedimentary history of the Cape Bojador continental margin, Northwestern Africa. In: Ryan, W.B.F., von Rad, U.J., et al. (Eds.), *Init Repts DSDP*, vol. 47(1), pp. 773–816.
- AUXINI (Departamento de Investigaciones Petrolíferas de AUXINI), 1969. Correlación estratigráfica de los sondeos perforados en el Sahara español. *Bol. Geol. Minero, Madrid*, vol. 83, pp. 235–251.
- Barrat, J.A., Keller, F., Amossé, J., Taylor, R.N., Nesbitt, R.W., Hirata, T., 1996. Determination of rare earth elements in sixteen silicate reference samples by ICP-MS after Tm addition and ion exchange separation. *Geostandard Newslett.* 20 (1), 133–139.
- Bau, M., 1999. Scavenging of dissolved yttrium and rare earths by precipitating iron oxyhydroxide: experimental evidence for Ce oxidation, Y-Ho fractionation and lanthanide tetrad effect. *Geochimica et Cosmochimica Acta* 63 (1), 67–77.
- Bau, M., Dulski, P., Moller, P., 1995. Yttrium and holmium in South Pacific seawater: vertical distribution and possible fractionation mechanisms. *chemieChemie der Erde-Geochemistry* 55, 1–15.
- Bauluz, B., Mayayo, M.J., Fernandez-Nieto, C., Gonzalez Lopez, J.M., 2000. Geochemistry of precambrian and paleozoic siliciclastic rocks from the Iberian range (NE Spain): implications for source-area weathering, sorting, provenance and tectonic setting. *Chem. Geol.* 168 (1–2), 135–150.
- Bayon, G., German, C.R., Boella, R.M., Milton, J.A., Taylor, R.N., Nesbitt, R.W., 2002. An improved method for extracting marine sediment fractions and its application to Sr and Nd isotopic analysis. *Chem. Geol.* 187 (3–4), 179–199.
- Bhatia, M.R., 1983. Plate tectonics and geochemical composition of sandstones. *J. Geol.* 91 (6), 611–627.
- Bhatia, M.R., 1984. Composition and classification of Paleozoic flysch mudrocks of eastern Australia: implications in provenance and tectonic setting interpretation. *Sediment. Geol.* 41 (2–4), 249–268.
- Bhatia, M.R., 1985. Rare earth element geochemistry of Australian Paleozoic graywackes and mudrocks: provenance and tectonic control. *Sediment. Geol.* 45 (1–2), 97–113.
- Bhatia, M.R., Crook, K.A.W., 1986. Trace element characteristics of graywackes and tectonic setting discrimination of sedimentary basins. *Contribut. Mineral. Petrol.* 92 (2), 181–193.
- Bock, B., McLennan, S.M., Hanson, N., 1994. Rare earth element redistribution and its effects on the neodymium isotope system in the Austin Glen Member of the Normanskill Formation, New York, USA. *Geochimica et Cosmochimica Acta* 58 (23), 5245–5253.
- Choubert, G., FaureMuret, A., Hottinger, L., 1966. Aperçu géologique du bassin côtier de Tarfaya. *Notes et Mem Serv Geol Maroc* 1, 7–106.
- Cohen, A.S., O'Nions, R.K., Siegenthaler, R., Griffin, W.L., 1988. Chronology of the pressure-temperature history recorded by a granulite terrain. *Contribut. Mineral. Petrol.* 98 (3), 303–311.
- Cole, J.M., Goldstein, S.L., deMenocal, P.B., Hemming, S.R., Grousset, F.E., 2009. Contrasting compositions of Saharan dust in the eastern Atlantic Ocean during the last deglaciation and African humid period. *Earth Planet. Sci. Lett.* 278 (3–4), 257–266.
- Cox, R., Lowe, D.R., Cullers, R.L., 1995. The influence of sediment recycling and basement composition on evolution of mudrock chemistry in the southwestern United States. *Geochimica et Cosmochimica Acta* 59 (14), 2919–2940.
- Cullers, R.L., 1994. The controls on the major and trace element variation of shales, siltstones, and sandstones of Pennsylvanian-Permian age from uplifted continental blocks in Colorado to platform sediment in Kansas, USA. *Geochimica et Cosmochimica Acta* 58 (22), 4955–4972.
- Cullers, R.L., 2000. The geochemistry of shales, siltstones and sandstones of Pennsylvanian-Permian age, Colorado, USA: implications for provenance and metamorphic studies. *Lithos* 51 (3), 181–203.
- Cullers, R.L., Basu, A., Suttner, L., 1988. Geochemical signature of provenance in sand-size material in soils and stream sediments near the Tobacco Root batholith, Montan, USA. *Chemical Geology* 70, 335–348.
- Cullers, R.L., Graf, J., 1983. Rare Earth Elements in Igneous Rocks of the Continental Crust: Intermediate and Silicic Rocks, or Petrogenesis. *Rare-Earth Geochemistry*, Elsevier, Amsterdam, pp. 275–312.
- Cullers, R.L., Podkovyrov, V.N., 2000. Geochemistry of the Mesoproterozoic Lakhanda shales in southeastern Yakutia, Russia: implications for mineralogical and provenance control and recycling. *Precambrian Res.* 104 (1–2), 77–93.
- DePaolo, D.J., 1980. Sources of continental crust: neodymium isotope evidence from the Sierra Nevada and peninsular ranges. *Science* 209 (4457), 684–687.
- DePaolo, D.J., 1981. Neodymium isotopes in the Colorado Front Range and crust-mantle evolution in the Proterozoic. *Nature* 291 (5812), 193–196.
- Dillon, R.S., Sougy, J.H.A., 1974. Geology of West Africa and Canary and Cape Verde Island. In: Nairn, A.E.M., Stehli, F.G. (Eds.), *The Ocean Basins and Margins*, 2. Plenum Press: The North Atlantic, New York, pp. 315–390.
- El Albani, A., Kuhnt, W., Luderer, F., Herbin, J.P., Caron, M., 1999. Palaeoenvironmental evolution of the Late Cretaceous sequence in the Tarfaya Basin (southwest of Morocco). *Geol. Soc., Lond., Special Publ.* 153 (1), 223–240.
- Feng, R., Kerrich, R., 1990. Geochemistry of fine-grained clastic sediments in the Archean Abitibi greenstone belt, Canada: implications for provenance and tectonic setting. *Geochimica et Cosmochimica Acta* 54 (4), 1061–1081.
- Frizon de Lamotte, D.F., Leturmy, P., Missenard, Y., Khomsi, S., Ruiz, G., Saddiqi, O., Guillocheau, F., Michard, A., 2009. Mesozoic and Cenozoic vertical movements in the Atlas system (Algeria, Morocco, Tunisia): an overview. *Tectonophysics* 475 (1), 9–28.
- Garbe-Schönberg, C.-D., 1993. Simultaneous determination of thirty seven trace elements in twenty eight international rock standards by ICP-MS. *Geostandard Newslett.* 17 (1), 81–97.
- Garver, J.I., Royce, P.R., Smick, T.A., 1996. Chromium and Nickel in shale of the Taconic Foreland; a case study for the provenance of fine-grained sediments with an ultramafic source. *J. Sediment. Res.* 66 (1), 100–106.
- Gertsch, B., Adatte, T., Keller, G., Tantawy, A.A.A.M., Berner, Z., Mort, H.P., Fleitmann, D., 2010. Middle and late Cenomanian oceanic anoxic events in shallow and deeper shelf environments of western Morocco. *Sedimentology* 57 (6), 1430–1462.
- Hassan, S., Ishiga, H., Roser, B.P., Dozen, K., Naka, T., 1999. Geochemistry of Permian-Triassic shales in the salt range, Pakistan: implications for provenance and tectonism at the Gondwana margin. *Chem. Geol.* 158 (3–4), 293–314.

- Helg, U., Burkhand, M., Carigt, S., Robert-Charrue, Ch., 2004. Folding and inversion tectonics in the Anti-Atlas of Morocco. *Tectonics* 23, 1–17.
- Hiscott, R.N., 1984. Ophiolitic source rocks for Taconic-Age flysch: trace-element evidence. *Geol. Soc. Am. Bull.* 95 (11), 1261–1267.
- Horwitz, E.P., Chiarizia, R., Dietz, M.L., 1992. A novel strontium-selective extraction chromatographic resin. *Solvent Extr. Ion Exchange* 10 (2), 313–336.
- Keller, G., Adatte, T., Berner, Z., Chellai, E.H., Stueben, D., 2008. Oceanic events and biotic effects of the Cenomanian-Turonian anoxic event, Tarfaya Basin, Morocco. *Cretaceous Res.* 29 (5–6), 976–994.
- Kolonc, S., Wagner, T., Forster, A., Damsté, J.S.S., Walsworth-Bell, B., Erba, E., Turgeon, S., Brumsack, H.-J., Chellai, E.H., Tsikos, H., Kuhnt, W., Kuypers, M.M.M., 2005. Black shale deposition on the northwest African Shelf during the Cenomanian/Turonian oceanic anoxic event. Climate coupling and global organic carbon burial. *Paleoceanography*, vol. 20, PA1006, PA1006, 2005, doi:10.1029/2003PA000950.
- Kuhnt, W., Holbourn, A., Gale, A., Chellai, E.H., Kennedy, W.J., 2009. Cenomanian sequence stratigraphy and Sea-Level fluctuations in the Tarfaya Basin (SW Morocco). *Geol. Soc. Am. Bull.* 121 (11–12), 1695–1710.
- Kuhnt, W., Luderer, F., Nederbragt, S., Thurow, J., Wagner, T., 2005. Orbital-scale record of the late Cenomanian–Turonian oceanic anoxic event (OAE-2) in the Tarfaya Basin (Morocco). *Int. J. Earth Sci.* 94 (1), 147–159.
- Kuhnt, W., Nederbragt, A., Leine, L., 1997. Cyclicity of Cenomanian-Turonian organic-carbon-rich sediments in the Tarfaya Atlantic Coastal Basin (Morocco). *Cretaceous Res.* 18 (4), 587–601.
- Lahondere, D., Thieblemont, D., et al., 2003. Notice explicative des cartes géologiques a 1/200.000 et 1/500.000 du nord de la Mauritanie, DMG, Ministère Mines Industrie, Nouakchott.
- Le Fèvre, B., Pin, C., 2005. A straightforward separation scheme for concomitant Lu–Hf and Sm–Nd isotope ratio and isotope dilution analysis. *Analytica Chimica Acta* 543 (1–2), 209–221.
- McCulloch, M.T., Wasserburg, G.J., 1978. Sm–Nd and Rb–Sr chronology of continental crust formation. *Science* 200 (4345), 1003–1011.
- McDaniel, D.K., Hemming, S.R., McLennan, S.M., Hanson, G.N., 1994. Resetting of neodymium isotopes and redistribution of REEs during sedimentary processes: the Early Proterozoic Chelmsford Formation, Sudbury Basin, Ontario, Canada. *Geochimica et Cosmochimica Acta* 58 (2), 931–941.
- McLennan, S.M., 1989. Rare earth elements in sedimentary rocks; influence of provenance and sedimentary processes. *Rev. Mineral. Geochem.* 21 (1), 169–200.
- McLennan, S.M., 2001. Relationships between the trace element composition of sedimentary rocks and upper continental crust. *Geochem. Geophys. Geosyst.* 2 (4), 2001. <http://dx.doi.org/10.1029/2000GC000109>.
- McLennan, S.M., Taylor, S.R., 1991. Sedimentary rocks and crustal evolution: tectonic setting and secular trends. *J. Geol.* 99 (1), 1–21.
- McLennan, S.M., Taylor, S.R., Eriksson, K.A., 1983. Geochemistry of Archean shales from the Pilbara Supergroup, Western Australia. *Geochimica et Cosmochimica Acta* 47 (7), 1211–1222.
- McLennan, S.M., Taylor, S.R., Hemming, S.R., 2006. Composition, differentiation and evolution of continental crust: constraints from sedimentary rocks and heat flow. In: Brown, M., Rushmer, T. (Eds.), *Evolution and Differentiation of The Continental Crust*. Cambridge University Press, Cambridge, pp. 92–134.
- McLennan, S.M., Taylor, S.R., McCulloch, T.M., Maynard, J.B., 1990. Geochemical and Nd–Sr isotopic composition of deep-sea turbidites: Crustal evolution and plate tectonic associations. *Geochimica et Cosmochimica Acta* 54 (7), 2015–2050.
- McLennan, S.M., Taylor, S.R., McDaniel, D.K., Hanson, G.N., 1993. Geochemical approaches to sedimentation, provenance and tectonics, in processing controlling the composition of clastic sediments. In: Johnson, M.J., Basu, A. (Eds.), *Special Publication Geological Society of America*, vol. 284, pp. 21–40.
- Mearns, E.W., Knarud, R., Raestad, N., Stanley, K.O., Stockbridge, C.P., 1989. Samarium–Neodymium isotope stratigraphy of the Lunde and Statfjord Formations of Snorre Oil Field, Northern North Sea. *J. Geol. Soc.* 146 (2), 217–228.
- Meyer, I., Davies, G.R., Stuut, J.B.W., Grain size control on Sr–Nd isotope provenance studies and impact on palaeoclimate reconstructions: an example from deep-sea sediments offshore NW Africa. *Geochem. Geophys. Geosyst.*, 12, 2011, Q03005. <http://dx.doi.org/10.1029/2010GC003355>.
- Michard, A., 1976. *Éléments de géologie marocaine*. Notes Mém Serv Géol Maroc 252, 408.
- Michard, A., Saddiqi, O., Chalouanand, A., Frozen de Lamotte, D., 2008. Continental Evolution: The Geology of Morocco. Structure, Stratigraphy, and Tectonics of the Africa-Atlantic-Mediterranean Triple. Springer-Verlag, Heidelberg, p. 443.
- Middelburg, J.J., van der Weijden, C.H., Woitiez, J.R.W., 1988. Chemical processes affecting the mobility of major, minor and trace elements during weathering of granitic rocks. *Chem. Geol.* 68 (3–4), 253–273.
- Mort, H.P., Adatte, T., Föllmi, K.B., Keller, G., Steinmann, P., Matera, V., Berner, Z., Stüben, D., 2007. Phosphorus and the roles of productivity and nutrient recycling during Oceanic Anoxic Event 2. *Geology* 35 (6), 483–486.
- Mort, H.P., Adatte, T., Keller, G., Bartels, D., Föllmi, K.B., Steinmann, P., Berner, Z., Chellai, E.H., 2008. Organic carbon deposition and phosphorus accumulation during Oceanic Anoxic Event 2 in Tarfaya, Morocco. *Cretaceous Res.* 29 (5–6), 1008–1023.
- Nesbitt, H.W., Markovics, G., Price, R.C., 1980. Chemical processes affecting alkalis and alkaline earths during continental weathering. *Geochimica et Cosmochimica Acta* 44 (11), 1659–1666.
- Nesbitt, H.W., Young, G.M., 1982. Early Proterozoic climates and plate motions inferred from major element chemistry of lutites. *Nature* 299 (5885), 715–717.
- Nesbitt, H.W., Young, G.M., McLennan, S.M., Keays, R.R., 1996. Effects of chemical weathering and sorting on the petrogenesis of siliciclastic sediments, with implications for provenance studies. *J. Geol.* 104 (5), 525–542.
- O’Nions, R.K., Hamilton, P.J., Hooker, P.J., 1983. A Nd isotope investigation of sediments related to crustal development in the British Isles. *Earth Planet. Sci. Lett.* 63 (2), 229–240.
- Ranke, U., von Rad, U., Wissmann, G., 1982. Stratigraphy, facies and tectonic development of on- and offshore Aaiun–Tarfaya Basin—a review. In: von Rad, U., Hinz, K., Sarnthein, M., Seibold, E. (Eds.), *Geology of the North West African Continental Margin*. Springer-Verlag, pp. 86–104.
- Ratschiller, L.K., 1970. Lithostratigraphy of the northern Spanish Sahara. *Memorie Museo Tridentino Sci Trento* 18 (1), 1–18.
- Roddaz, M., Said, A., Guillot, S., Antoine, P.O., Montel, J.-M., Martin, F., Darrozes, J., 2011. Provenance of Cenozoic sedimentary rocks from the Sulaiman Fold and Thrust Belt, Pakistan: Implications for the Palaeogeography of the Indus Drainage System. *J. Geol. Soc.* 168 (2), 499–516.
- Roser, B.P., Korsch, R.J., 1986. Determination of tectonic setting of sandstone-mudstone suites using SiO₂ content and K₂O/Na₂O ratio. *J. Geol.* 94 (5), 635–650.
- Roser, B.P., Korsch, R.J., 1988. Provenance signatures of sandstone-mudstone suites determined using discriminant function analysis of major-element data. *Chem. Geol.* 67 (1–2), 119–139.
- Ruiz, G.M.H., Sebti, S., Negro, F., Saddiqi, O., Frizon de Lamotte, D., Stockli, D., Foeken, J., Stuart, F., Barbarand, J., Schaefer, J.P., 2010. From central Atlantic continental rift to Neogene uplift – western Anti-Atlas (Morocco). *Terra Nova* 23 (1), 35–41.
- Schofield, D.I., Gillespie, M.R., 2007. A tectonic interpretation of “Eburnean terraneterrain” outliers in the Reguibat Shield, Mauritania. *J. African Earth Sci.* 49 (4–5), 179–186.
- Schofield, D.I., Horstwood, M.S.A., Pitfield, P.E.J., Crowley, Q.G., Wilkinson, A.F., Sidaty, H.C.O., 2006. Timing and Kinematics of Eburnean Tectonics in the Central Reguibat Shield, Mauritania. *J. Geol. Soc.* 163 (3), 549–560.
- Sehrt, M., Glasmacher, U.A., Stockli, D., Kluth, O., Schober, J., Jabour, H., Lahsini, S., Boutib, L., 2011. Thermal and inversion history of the Tarfaya basin and uplift and exhumation history of a potential source area, the western Anti-Atlas, assessed by low temperature thermochronology. In: Paper presented at MAPG-AAPG 2nd international convention, conference and exhibition, Marrakech, Morocco.
- Soulaimani, A., Le Corre, C., Farazdaq, R., 1997. Deformation hercynienne et tectonique socle/couverture dans le domaine du Bas-Draa (Anti-Atlas occidental, Maroc). *J. African Earth Sci.* 24, 271–284.
- Steiger, R.H., Jäger, E., 1977. Subcommittee on geochronology: convention on the use of decay constants in geo- and cosmochronology. *Earth Planet. Sci. Lett.* 36 (3), 359–362.
- Tanaka, T., Togashi, S., Kamioka, H., Amakawa, H., Kagami, H., Hamamoto, T., Yuhara, M., Orihashi, Y., Yoneda, S., Shimizu, H., Kunimaru, T., Takahashi, K., Yanagi, T., Nakano, T., et al., 2000. JNdi-1: a neodymium isotopic reference in consistency with LaJolla neodymium. *Chem. Geol.* 168 (3–4), 279–281.
- Taylor, S.R., McLennan, S.M., 1985. *The Continental Crust: Its Composition and Evolution*. Blackwell, Oxford, p. 312.
- Tütken, T., Eisenhauer, A., Wiegand, B., Hansen, B.T., 2002. Glacial-interglacial cycles in Sr and Nd isotopic composition of Arctic marine sediments triggered by the Svalbard/Barents Sea ice sheet. *Mar. Geol.* 182, 351–372.
- Vail, P., Miltchum Jr. R.M., Thompson III, S., 1977. Global cycles of relative changes of sea level. In: Vail, P.R. et al. (Eds.), *Seismic Stratigraphy and Global Changes of Sea Level*. American Association of Petroleum Geology Memoriam, vol. 26, pp. 83–98.
- Wade, B.P., Hand, M., Barovich, K.M., 2005. Nd isotopic and geochemical constraints on provenance of sedimentary rocks in the eastern Officer Basin, Australia: implications for the duration of the intracratonic Petermann Orogeny. *J. Geol. Soc.* 162 (3), 513–530.
- Wrafter, J.P., Graham, J.R., 1989. Short Paper: Ophiolitic detritus in the Ordovician sediments of South Mayo, Ireland. *J. Geol. Soc.* 146 (2), 213–215.
- Wronkiewicz, D.J., Condie, K.C., 1987. Geochemistry of Archean shales from the Witwatersrand Supergroup, South Africa: Source-area weathering and provenance. *Geochimica et Cosmochimica Acta* 51 (9), 2401–2416.
- Wronkiewicz, D.J., Condie, K.C., 1990. Geochemistry and mineralogy of sediments from the Ventersdorp and Transvaal Supergroups, South Africa: Cratonic evolution during the early Proterozoic. *Geochimica et Cosmochimica Acta* 54 (2), 343–354.
- Xie, S., Wu, Y., Gao, S., Liu, X., Zhou, L., Zhao, L., Hu, Z., 2012. Sr–Nd isotopic and geochemical constraints on provenance of late Paleozoic to early Cretaceous sedimentary rocks in the Western Hills of Beijing, North China: Implications for the uplift of the northern North China Craton. *Sediment. Geol.* 245–246 (0), 17–28.
- Zhang, K.J., Zhang, Y.X., Li, B., Zhong, L.F., 2007. Nd isotopes of siliciclastic rocks from Tibet, western China: constraints on provenance and pre-Cenozoic tectonic evolution. *Earth Planet. Sci. Lett.* 256 (3–4), 604–616.
- Zimmermann, U., Bahlgel, H., 2003. Provenance analysis and tectonic setting of the Ordovician clastic deposits in the southern Puna Basin, NW Argentina. *Sedimentology* 50 (6), 1079–1104.